

# Constraints on the non-standard interaction in propagation from atmospheric neutrinos

---

**Shinya Fukasawa, Osamu Yasuda**

*Department of Physics, Tokyo Metropolitan University, Minami-Osawa, Hachioji, Tokyo 192-0397, Japan*

**ABSTRACT:** The sensitivity of the atmospheric neutrino experiments to the non-standard flavor-dependent interaction in neutrino propagation is studied under the assumption that the only nonvanishing components of the non-standard matter effect are the electron and tau neutrino components  $\epsilon_{ee}$ ,  $\epsilon_{e\tau}$ ,  $\epsilon_{\tau\tau}$  and that the tau-tau component satisfies the constraint  $\epsilon_{\tau\tau} = |\epsilon_{e\tau}|^2 / (1 + \epsilon_{ee})$  which is suggested from the high energy behavior for atmospheric neutrino data. It is shown that the Superkamiokande (SK) data for 4438 days constrains  $|\tan \beta| \equiv |\epsilon_{e\tau}/(1 + \epsilon_{ee})| \lesssim 0.8$  at  $2.5\sigma$  (98.8%) CL whereas the future Hyperkamiokande experiment for the same period of time as SK will constrain as  $|\tan \beta| \lesssim 0.3$  at  $2.5\sigma$  CL from the energy rate analysis and the energy spectrum analysis will give even tighter bounds on  $\epsilon_{ee}$  and  $|\epsilon_{e\tau}|$ .

**KEYWORDS:** Neutrino oscillations, Atmospheric neutrinos, Nonstandard interactions

---

## Contents

<b>1</b>	<b>introduction</b>	<b>1</b>
<b>2</b>	<b>The constraint of the Superkamiokande atmospheric neutrino experiment on <math>\epsilon_{ee}</math> and <math> \epsilon_{e\tau} </math></b>	<b>3</b>
<b>3</b>	<b>Sensitivity of the Hyperkamiokande atmospheric neutrino experiment to <math>\epsilon_{ee}</math> and <math> \epsilon_{e\tau} </math></b>	<b>6</b>
3.1	The case with the standard oscillation scenario	6
3.2	The case in the presence of NSI	13
<b>4</b>	<b>Conclusions</b>	<b>14</b>

---

## 1 introduction

From the experiments with solar, atmospheric, reactor and accelerator neutrinos it is now established that neutrinos have masses and mixings [1]. Neutrino oscillations in the standard three-flavor scheme are described by three mixing angles,  $\theta_{12}$ ,  $\theta_{13}$ ,  $\theta_{23}$ , one CP phase  $\delta$ , and two independent mass-squared differences,  $\Delta m_{21}^2$  and  $\Delta m_{31}^2$ . The sets of the parameters ( $\Delta m_{21}^2$ ,  $\theta_{12}$ ) and ( $|\Delta m_{31}^2|$ ,  $\theta_{23}$ ) were determined by the solar neutrino experiments and the KamLAND experiment, and by atmospheric and long baseline neutrino experiments, respectively.  $\theta_{13}$  was determined by the reactor experiments and the long baseline experiments [1]. The only oscillation parameters which are still undetermined are the value of the CP phase  $\delta$  and the sign of  $\Delta m_{31}^2$  (the mass hierarchy). In the future neutrino long-baseline experiments with intense neutrino beams the sign of  $\Delta m_{31}^2$  and  $\delta$  are expected to be determined [2, 3]. As in the case of B factories [4, 5], such high precision measurements will enable us to search for deviation from the standard three-flavor oscillations (see, e.g., Ref. [6]). Among such possibilities, in this paper, we will discuss the effective non-standard neutral current flavor-dependent neutrino interaction with matter [7–9] given by

$$\mathcal{L}_{\text{eff}}^{\text{NSI}} = -2\sqrt{2}\epsilon_{\alpha\beta}^{fP}G_F(\bar{\nu}_\alpha\gamma_\mu P_L\nu_\beta)(\bar{f}\gamma^\mu Pf'), \quad (1.1)$$

where  $f$  and  $f'$  stand for fermions (the only relevant ones are electrons, u and d quarks),  $G_F$  is the Fermi coupling constant, and  $P$  stands for a projection operator that is either  $P_L \equiv (1 - \gamma_5)/2$  or  $P_R \equiv (1 + \gamma_5)/2$ . If the interaction (1.1) exists, then the standard matter effect [7, 10] is modified. We will discuss atmospheric neutrinos which go through the Earth, so we make an approximation that the number densities of electrons ( $N_e$ ), protons, and neutrons are equal.<sup>1</sup> Defining  $\epsilon_{\alpha\beta} \equiv \sum_P (\epsilon_{\alpha\beta}^{eP} + 3\epsilon_{\alpha\beta}^{uP} + 3\epsilon_{\alpha\beta}^{dP})$ , the hermitian

---

<sup>1</sup> This assumption is not valid in other environments, e.g., in the Sun.

$3 \times 3$  matrix of the matter potential becomes

$$\mathcal{A} \equiv A \begin{pmatrix} 1 + \epsilon_{ee} & \epsilon_{e\mu} & \epsilon_{e\tau} \\ \epsilon_{\mu e} & \epsilon_{\mu\mu} & \epsilon_{\mu\tau} \\ \epsilon_{\tau e} & \epsilon_{\tau\mu} & \epsilon_{\tau\tau} \end{pmatrix}, \quad (1.2)$$

where  $A \equiv \sqrt{2}G_F N_e$  stands for the matter effect due to the charged current interaction in the standard case. With this matter potential, the Dirac equation for neutrinos in matter becomes

$$i \frac{d}{dx} \begin{pmatrix} \nu_e(x) \\ \nu_\mu(x) \\ \nu_\tau(x) \end{pmatrix} = [U \text{diag}(0, \Delta E_{21}, \Delta E_{31}) U^{-1} + \mathcal{A}] \begin{pmatrix} \nu_e(x) \\ \nu_\mu(x) \\ \nu_\tau(x) \end{pmatrix}, \quad (1.3)$$

where  $U$  is the leptonic mixing matrix defined by

$$U \equiv \begin{pmatrix} c_{12}c_{13} & s_{12}c_{13} & s_{13}e^{-i\delta} \\ -s_{12}c_{23} - c_{12}s_{23}s_{13}e^{i\delta} & c_{12}c_{23} - s_{12}s_{23}s_{13}e^{i\delta} & s_{23}c_{13} \\ s_{12}s_{23} - c_{12}c_{23}s_{13}e^{i\delta} & -c_{12}s_{23} - s_{12}c_{23}s_{13}e^{i\delta} & c_{23}c_{13} \end{pmatrix}, \quad (1.4)$$

and  $\Delta E_{jk} \equiv \Delta m_{jk}^2/2E \equiv (m_j^2 - m_k^2)/2E$ ,  $c_{jk} \equiv \cos \theta_{jk}$ ,  $s_{jk} \equiv \sin \theta_{jk}$ .

Constraints on  $\epsilon_{\alpha\beta}$  from various neutrino experiments have been discussed in Refs. [11–19]. Since the coefficients  $\epsilon_{\alpha\beta}$  in Eq. (1.2) are given by  $\epsilon_{\alpha\beta} \sim \epsilon_{\alpha\beta}^e + 3\epsilon_{\alpha\beta}^u + 3\epsilon_{\alpha\beta}^d$ , considering the constraints by Refs. [11–19], we have the following limits [20] at 90%CL:

$$\begin{pmatrix} |\epsilon_{ee}| < 4 \times 10^0 & |\epsilon_{e\mu}| < 3 \times 10^{-1} & |\epsilon_{e\tau}| < 3 \times 10^0 \\ & |\epsilon_{\mu\mu}| < 7 \times 10^{-2} & |\epsilon_{\mu\tau}| < 3 \times 10^{-1} \\ & & |\epsilon_{\tau\tau}| < 2 \times 10^1 \end{pmatrix}. \quad (1.5)$$

From Eq. (1.5) we observe that the bounds on  $\epsilon_{ee}$ ,  $\epsilon_{e\tau}$  and  $\epsilon_{\tau\tau}$  are much weaker than those on  $\epsilon_{\alpha\mu}$  ( $\alpha = e, \mu, \tau$ ).

On the other hand, the non-standard interaction (NSI) with components  $\epsilon_{\alpha\beta}$  ( $\alpha, \beta = e, \tau$ ) must be consistent with the high-energy atmospheric neutrino data. It was pointed out in Refs. [21, 22] that the relation

$$|\epsilon_{e\tau}|^2 \simeq \epsilon_{\tau\tau} (1 + \epsilon_{ee}), \quad (1.6)$$

should hold for the matter potential (1.2) to be consistent with the high-energy atmospheric neutrino data, which suggest the behavior of the disappearance oscillation probability

$$1 - P(\nu_\mu \rightarrow \nu_\mu) \sim \sin^2 2\theta_{\text{atm}} \sin^2 \left( \frac{\Delta m_{\text{atm}}^2 L}{4E} \right) \propto \frac{1}{E^2}, \quad (1.7)$$

where  $\sin^2 2\theta_{\text{atm}}$  and  $\Delta m_{\text{atm}}^2$  are the oscillation parameters in the two-flavor formalism. In Ref. [23] it was shown that, in the high-energy behavior of the disappearance oscillation probability

$$1 - P(\nu_\mu \rightarrow \nu_\mu) \simeq c_0 + \frac{c_1}{E} + \mathcal{O}\left(\frac{1}{E^2}\right), \quad (1.8)$$

in the presence of the matter potential (1.2),  $|c_0| \ll 1$  and  $|c_1| \ll 1$  imply  $\epsilon_{e\mu} \simeq \epsilon_{\mu\mu} \simeq \epsilon_{\mu\tau} \simeq 0$  and  $\epsilon_{\tau\tau} \simeq |\epsilon_{e\tau}|^2 / (1 + \epsilon_{ee})$ .

Taking into account the various constraints described above, in the present paper we take the ansatz

$$\mathcal{A} = A \begin{pmatrix} 1 + \epsilon_{ee} & 0 & \epsilon_{e\tau} \\ 0 & 0 & 0 \\ \epsilon_{e\tau}^* & 0 & |\epsilon_{e\tau}|^2 / (1 + \epsilon_{ee}) \end{pmatrix}, \quad (1.9)$$

and analyze the sensitivity to the parameters  $\epsilon_{\alpha\beta}$  ( $\alpha, \beta = e, \tau$ ) of the atmospheric neutrino experiment at Superkamiokande and the future Hyperkamiokande (HK) facility [24].

The constraints on  $\epsilon_{ee}$  and  $\epsilon_{e\tau}$  from the atmospheric neutrino has been discussed in Refs [25–27] with the ansatz different from ours.

The effect of the non-standard interaction in propagation for solar neutrinos has also been discussed in Refs. [15, 18, 19, 28, 29], and Refs. [19] and [29] give a constraint  $-0.06 < \epsilon_{e\tau}^{dV} \sin \theta_{23} < 0.41$  (at 90%CL) and  $|\epsilon_{e\tau}^{dV}| \lesssim 0.4$  (at  $\Delta\chi^2 = 4$  for 2 d.o.f.), respectively.

The sensitivity of the ongoing long-baseline experiments to the non-standard interaction in propagation was studied for MINOS in Refs. [30–34], and for OPERA in Refs. [35, 36]. As for the future long-baseline experiments, the sensitivity of the reactor and super-beam experiments was discussed in Ref. [37], that of the T2KK experiment was studied in Refs. [23, 38], and that of neutrino factories [6] was discussed by many authors [39–46].

The paper is organized as follows. In sect. 2, we analyze the SK atmospheric neutrino data and give the constraints on the parameters  $\epsilon_{\alpha\beta}$  ( $\alpha, \beta = e, \tau$ ) from the SK atmospheric neutrino data. In sect. 3, we discuss the sensitivity to  $\epsilon_{\alpha\beta}$  ( $\alpha, \beta = e, \tau$ ) of the future Hyperkamiokande atmospheric neutrino experiment. In sect. 4, we draw our conclusions.

## 2 The constraint of the Superkamiokande atmospheric neutrino experiment on $\epsilon_{ee}$ and $|\epsilon_{e\tau}|$

In this section we discuss the constraint of the SK atmospheric neutrino experiment on the non-standard interaction in propagation with the ansatz (1.9). The independent degrees of freedom in addition to those in the standard oscillation scenario are  $\epsilon_{ee}$ ,  $|\epsilon_{e\tau}|$  and  $\arg(\epsilon_{e\tau})$ .

The SK atmospheric neutrino data we analyze here is those in Ref. [47] for 4438 days. In Ref. [47], the contained events, the partially contained events and the upward going  $\mu$  events are divided into a few categories. Since we have been unable to reproduce all their results of the Monte Carlo simulation, we have combined the two sub-GeV  $\mu$ -like data set in one, the two multi-GeV e-like in one, the two partially contained event data set and the multi-GeV  $\mu$ -like in one, and the three upward going  $\mu$  in one. Ref. [47] gives information on the ten zenith angle bins, while that on the energy bins is not given, so we perform analysis with the ten zenith angle bins and one energy bin, i.e., we perform the rate analysis as far as the energy is concerned.

The analysis was performed with the codes which were used in Refs. [48–50].  $\chi^2$  is defined as

$$\chi^2 = \min_{\theta_{23}, |\Delta m_{32}^2|, \delta, \arg(\epsilon_{e\tau})} (\chi_{\text{sub-GeV}}^2 + \chi_{\text{multi-GeV}}^2 + \chi_{\text{upward}}^2). \quad (2.1)$$

In eq. (2.1)  $\chi^2$  for the sub-GeV, multi-GeV, and upward going  $\mu$  events are defined by

$$\begin{aligned} \chi_{\text{sub-GeV}}^2 = \min_{\alpha_s, \beta's} & \left[ \frac{\beta_{s1}^2}{\sigma_{\beta s1}^2} + \frac{\beta_{s2}^2}{\sigma_{\beta s2}^2} + \sum_{j=1}^{10} \left\{ \frac{1}{n_j^s(e)} \left[ \alpha_s \left( 1 - \frac{\beta_{s1}}{2} + \frac{\beta_{s2}}{2} \right) N_j^s(\nu_e \rightarrow \nu_e) \right. \right. \right. \\ & + \alpha_s \left( 1 + \frac{\beta_{s1}}{2} + \frac{\beta_{s2}}{2} \right) N_j^s(\nu_\mu \rightarrow \nu_e) \\ & + \alpha_s \left( 1 - \frac{\beta_{s1}}{2} - \frac{\beta_{s2}}{2} \right) N_j^s(\bar{\nu}_e \rightarrow \bar{\nu}_e) \\ & \left. \left. \left. + \alpha_s \left( 1 + \frac{\beta_{s1}}{2} - \frac{\beta_{s2}}{2} \right) N_j^s(\bar{\nu}_\mu \rightarrow \bar{\nu}_e) - n_j^s(e) \right]^2 \right. \right. \\ & + \frac{1}{n_j^s(\mu)} \left[ \alpha_s \left( 1 - \frac{\beta_{s1}}{2} + \frac{\beta_{s2}}{2} \right) N_j^s(\nu_e \rightarrow \nu_\mu) \right. \\ & + \alpha_s \left( 1 + \frac{\beta_{s1}}{2} + \frac{\beta_{s2}}{2} \right) N_j^s(\nu_\mu \rightarrow \nu_\mu) \\ & + \alpha_s \left( 1 - \frac{\beta_{s1}}{2} - \frac{\beta_{s2}}{2} \right) N_j^s(\bar{\nu}_e \rightarrow \bar{\nu}_\mu) \\ & \left. \left. \left. + \alpha_s \left( 1 + \frac{\beta_{s1}}{2} - \frac{\beta_{s2}}{2} \right) N_j^s(\bar{\nu}_\mu \rightarrow \bar{\nu}_\mu) - n_j^s(\mu) \right]^2 \right] \right\}, \end{aligned} \quad (2.2)$$

$$\begin{aligned} \chi_{\text{multi-GeV}}^2 = \min_{\alpha_m, \beta'm} & \left[ \frac{\beta_{m1}^2}{\sigma_{\beta m1}^2} + \frac{\beta_{m2}^2}{\sigma_{\beta m2}^2} + \sum_{j=1}^{10} \left\{ \frac{1}{n_j^m(e)} \left[ \alpha_s \left( 1 - \frac{\beta_{m1}}{2} + \frac{\beta_{m2}}{2} \right) N_j^m(\nu_e \rightarrow \nu_e) \right. \right. \right. \\ & + \alpha_s \left( 1 + \frac{\beta_{m1}}{2} + \frac{\beta_{m2}}{2} \right) N_j^m(\nu_\mu \rightarrow \nu_e) \\ & + \alpha_s \left( 1 - \frac{\beta_{m1}}{2} - \frac{\beta_{m2}}{2} \right) N_j^m(\bar{\nu}_e \rightarrow \bar{\nu}_e) \\ & \left. \left. \left. + \alpha_s \left( 1 + \frac{\beta_{m1}}{2} - \frac{\beta_{m2}}{2} \right) N_j^m(\bar{\nu}_\mu \rightarrow \bar{\nu}_e) - n_j^m(e) \right]^2 \right. \right. \\ & + \frac{1}{n_j^m(\mu)} \left[ \alpha_s \left( 1 - \frac{\beta_{m1}}{2} + \frac{\beta_{m2}}{2} \right) N_j^m(\nu_e \rightarrow \nu_\mu) \right. \\ & + \alpha_s \left( 1 + \frac{\beta_{m1}}{2} + \frac{\beta_{m2}}{2} \right) N_j^m(\nu_\mu \rightarrow \nu_\mu) \\ & + \alpha_s \left( 1 - \frac{\beta_{m1}}{2} - \frac{\beta_{m2}}{2} \right) N_j^m(\bar{\nu}_e \rightarrow \bar{\nu}_\mu) \\ & \left. \left. \left. + \alpha_s \left( 1 + \frac{\beta_{m1}}{2} - \frac{\beta_{m2}}{2} \right) N_j^m(\bar{\nu}_\mu \rightarrow \bar{\nu}_\mu) - n_j^m(\mu) \right]^2 \right] \right\}, \end{aligned} \quad (2.3)$$

$$\begin{aligned} \chi_{\text{upward}}^2 = \min_{\alpha_u} & \left\{ \frac{\alpha_u^2}{\sigma_\alpha^2} + \sum_{j=1}^{10} \frac{1}{n_j^u(\mu)} \left[ \alpha_u N_j^u(\nu_e \rightarrow \nu_\mu) + \alpha_u N_j^u(\nu_\mu \rightarrow \nu_\mu) \right. \right. \\ & \left. \left. + \alpha_u N_j^u(\bar{\nu}_e \rightarrow \bar{\nu}_\mu) + \alpha_u N_j^u(\bar{\nu}_\mu \rightarrow \bar{\nu}_\mu) - n_j^u(\mu) \right]^2 \right\}. \end{aligned}$$

The summation on  $j$  runs over the ten zenith angle bins for each  $\chi^2$ ,  $n_j^a(\alpha)$  ( $a=s, m$ ,

$u; \alpha = e, \mu$ ) stands for the neutrino *and* antineutrino data of the numbers of the sub-GeV, multi-GeV, and upward going  $\mu$  events,  $N_j^a(\nu_\alpha \rightarrow \nu_\beta)$  ( $N_j^a(\bar{\nu}_\alpha \rightarrow \bar{\nu}_\beta)$ ) stands for the theoretical prediction for the number of  $\ell_\beta$ -like events ( $\ell_\beta = e, \mu$ ) which is produced from  $\nu_\beta$  ( $\bar{\nu}_\beta$ ) that originates from  $\nu_\alpha$  ( $\bar{\nu}_\alpha$ ) through the oscillation process  $\nu_\alpha \rightarrow \nu_\beta$  ( $\bar{\nu}_\alpha \rightarrow \bar{\nu}_\beta$ ), and it is expressed as the product of the oscillation probability  $P(\nu_\alpha \rightarrow \nu_\beta)$  ( $P(\bar{\nu}_\alpha \rightarrow \bar{\nu}_\beta)$ ), the flux  $F(\nu_\alpha)$  ( $F(\bar{\nu}_\alpha)$ ), the cross section, the number of the targets and the detection efficiency.  $\alpha_a$  ( $a = s, m, u$ ) stands for the uncertainty in the overall flux normalization for the sub-GeV, multi-GeV, and upward going  $\mu$  events,  $\beta_{a1}$  ( $\beta_{a2}$ ) stands for the uncertainty in the relative normalization between  $\nu_e$  -  $\nu_\mu$  flux ( $\nu$  -  $\bar{\nu}$  flux) for the sub-GeV ( $a = s$ ) and multi-GeV ( $a = m$ ) events, respectively. It is understood that  $\chi^2$  is minimized with respect to  $\alpha_s, \beta_{sk}$  ( $k = 1, 2$ ),  $\alpha_m, \beta_{mk}$  ( $k = 1, 2$ ),  $\alpha_u$ . We have put the systematic errors

$$\sigma_{\beta s1} = \sigma_{\beta m1} = 0.03, \sigma_{\beta s2} = \sigma_{\beta m2} = 0.05, \sigma_\alpha = 0.2 \quad (2.4)$$

and we have assumed that  $\alpha_s$  and  $\alpha_m$  for the contained events are free parameters as in Ref. [51]. We have omitted the other uncertainties, such as the  $E_\nu$  spectral index, the relative normalization between PC and FC and up-down correlation, etc., for simplicity. In Eq. (2.1) the sum of each  $\chi^2$  is optimized with respect the mixing angle  $\theta_{23}$ , the mass squared difference  $|\Delta m_{32}^2|$ , the Dirac CP phase  $\delta$  and the phase  $\arg(\epsilon_{e\tau})$  of the parameter  $\epsilon_{e\tau}$ . The other oscillation parameters give little effect on  $\chi^2$ , so we have fixed them as  $\sin^2 2\theta_{12} = 0.86$ ,  $\sin^2 2\theta_{13} = 0.1$  and  $\Delta m_{21}^2 = 7.6 \times 10^{-5} \text{ eV}^2$ .

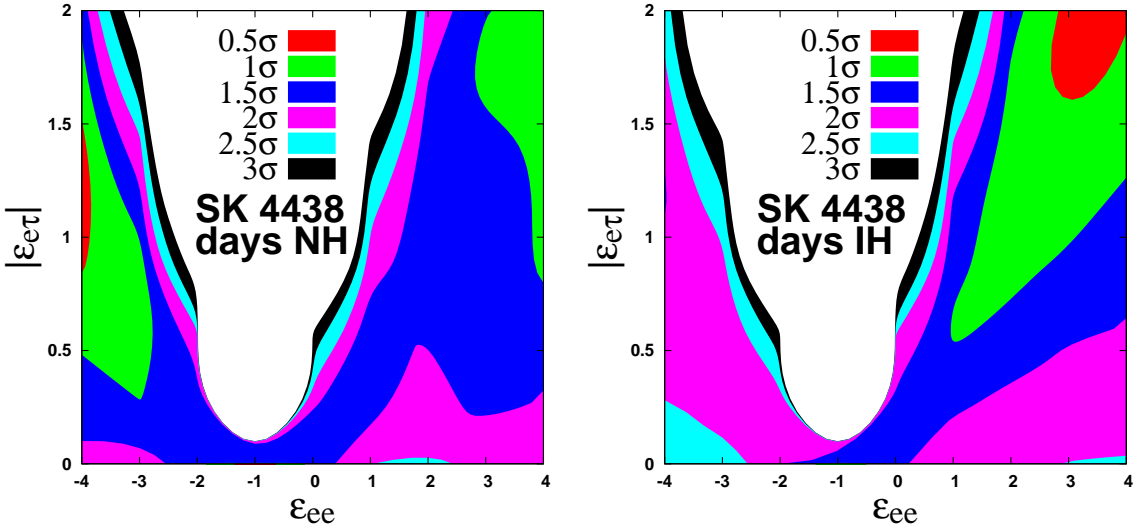


**Figure 1.** The allowed region in the  $(\epsilon_{ee}, |\epsilon_{e\tau}|)$  plane from the SK atmospheric neutrino data for a normal mass hierarchy (left panel) and for an inverted mass hierarchy (right panel).

The result for the Superkamiokande data for 4438 days is given in Fig. 1. The best-fit point for the normal (inverted) hierarchy is  $(\epsilon_{ee}, |\epsilon_{e\tau}|) = (-1.0, 0.0)$  ( $(3.0, 1.7)$ ) and the value of  $\chi^2$  at this point is 79.0 (78.6) for 50 degrees of freedom, and goodness of fit is 2.8 (2.7)  $\sigma$ CL, respectively. The best-fit point is different from the standard case  $(\epsilon_{ee}, |\epsilon_{e\tau}|) =$

(0, 0), and this may be not only because we have been unable to reproduce the Monte Carlo simulation by the Superkamiokande group, but also because we use only the information on the energy rate and the sensitivity to NSI is lost due to the destructive phenomena between the lower and higher energy bins (See the discussions in subsect. 3.1). The difference of the value of  $\chi^2$  for the standard case and that for the best-fit point for the normal (inverted) hierarchy is  $\Delta\chi^2 = 2.7$  (3.4) for 2 degrees of freedom ( $1.1\sigma$ CL ( $1.3\sigma$ CL)), respectively, and the standard case is certainly acceptable for the both mass hierarchies in our analysis. From the Fig. 1 we can read off the allowed region for  $|\tan\beta| \equiv |\epsilon_{e\tau}|/|1 + \epsilon_{ee}|$ , and we conclude that the allowed region for  $|\tan\beta|$  is approximately

$$|\tan\beta| \equiv \frac{|\epsilon_{e\tau}|}{|1 + \epsilon_{ee}|} \lesssim 0.8 \quad \text{at } 2.5\sigma\text{CL}.$$

### 3 Sensitivity of the Hyperkamiokande atmospheric neutrino experiment to $\epsilon_{ee}$ and $|\epsilon_{e\tau}|$

In this section we discuss the potential sensitivity of HK to  $\epsilon_{ee}$  and  $|\epsilon_{e\tau}|$ . Here we assume for simplicity that the the Hyperkamiokande detector has the same detection efficiencies as those of SK, and that the fiducial volume of HK is twenty times as large as that of SK. Since HK is a future experiment, the simulated numbers of events are used as “the experimental data”, and we vary  $\epsilon_{ee}$  and  $\epsilon_{e\tau}$  as well as the standard oscillation parameters trying to fit to “the experimental data”. Here we perform an analysis on the assumption that we know the mass hierarchy, because some hint on the mass hierarchy is expected to be available at some confidence level by the time HK will accumulate the atmospheric neutrino data for twenty years.

Since “the experimental data” are the simulated numbers of events, we can perform a energy spectrum analysis, assuming that the detection efficiency etc. are all equal among neutrinos and antineutrinos. Before we study the sensitivity to NSI, as a benchmark of our analysis, we have investigated the significance of the wrong mass hierarchy with our code, assuming the standard oscillation scenario and using different numbers of the energy bins. By comparing our result with the one in Ref. [24], we have found that our analysis on the mass hierarchy gives a result similar to that in Ref. [24], when we work with two energy bins in the contained events (the sub-GeV and multi-GeV events) and the systematic errors which are slightly different from those in Ref. [24]. We have checked that the sensitivity to NSI is not affected significantly by changing the systematic errors. As for the upward going  $\mu$  events, since our ansatz (1.9) is taken in such a way that the oscillation probability with  $\epsilon_{\alpha\beta}$  ( $\alpha, \beta = e, \tau$ ) approaches to the one with the standard scenario in the high energy limit, the upward going  $\mu$  events are expected to give a small contribution to the significance of NSI. So in the case of the energy spectrum analysis we will work with two energy bins in the contained events and a single energy bin in the upward going  $\mu$  events.

#### 3.1 The case with the standard oscillation scenario

First of all, let us discuss the case where “the experimental data” is the one obtained with the standard oscillation scenario. The values of the oscillation parameters which are used

to obtain “the experimental data” are the following<sup>2</sup>:

$$\begin{aligned}\Delta\bar{m}_{31}^2 &= 2.5 \times 10^{-3} \text{eV}^2, \sin^2\bar{\theta}_{23} = 0.5, \bar{\delta} = 0, \\ \sin^2 2\bar{\theta}_{12} &= 0.86, \sin^2 2\bar{\theta}_{13} = 0.1, \Delta\bar{m}_{21}^2 = 7.6 \times 10^{-5} \text{eV}^2.\end{aligned}\quad (3.1)$$

As in the case of the analysis of the SK data, we vary the oscillation parameters  $\theta_{23}$ ,  $|\Delta m_{32}^2|$ ,  $\delta$  and  $\arg(\epsilon_{e\tau})$  while fixing the other oscillation parameters  $\sin^2 2\theta_{12} = 0.86$ ,  $\sin^2 2\theta_{13} = 0.1$  and  $\Delta m_{21}^2 = 7.6 \times 10^{-5} \text{eV}^2$ .

In the energy rate analysis,  $\chi^2$  is the same as (2.1) where the numbers of events are calculated with the standard oscillation scenario with  $\bar{\theta}_{jk}$ ,  $\Delta\bar{m}_{jk}^2$  and  $\bar{\delta}$  given by Eq. (3.1), and we have assumed that all the systematic errors except  $\sigma_{\beta m2}$  are the same as those in Eq. (2.4) in the analysis of SK data.  $\sigma_{\beta m2} = 0.16$ , which is the uncertainty in the relative normalization between the  $\nu$  -  $\bar{\nu}$  flux, was chosen because this value was used in the energy spectrum analysis on the significance of the wrong mass hierarchy to give the result close to that in Ref. [24]. (See the discussions below.)

In the spectrum analysis, on the other hand,  $\chi^2_{\text{sub-GeV}}$  and  $\chi^2_{\text{multi-GeV}}$  are replaced by

---

<sup>2</sup> To distinguish the oscillation parameters for the “the experimental data” ( $n_{A_j}^a(\ell)$  ( $j = 1, \dots, 10; A = L, H; a = s, m; \ell = e, \mu$ ), etc.) and those for the numbers of events ( $N_{A_j}^a(\nu_\alpha \rightarrow \nu_\beta)$  ( $j = 1, \dots, 10; A = L, H; a = s, m; \alpha, \beta = e, \mu$ ), etc.) for fitting, the parameters with a bar denote those for “the experimental data”, whereas those without a bar denote the parameters for the numbers of events for fitting.

$$\begin{aligned}
& \chi^2_{\text{sub-GeV}} \\
&= \min_{\alpha_s, \beta's, \gamma's} \left[ \frac{\beta_{s1}^2}{\sigma_{\beta s1}^2} + \frac{\beta_{s2}^2}{\sigma_{\beta s2}^2} + \frac{\gamma_{L1}^2}{\sigma_{\gamma L1}^2} + \frac{\gamma_{L2}^2}{\sigma_{\gamma L2}^2} + \frac{\gamma_{H1}^2}{\sigma_{\gamma H1}^2} + \frac{\gamma_{H2}^2}{\sigma_{\gamma H2}^2} \right. \\
&\quad + \sum_{A=L,H} \sum_{j=1}^{10} \left\{ \frac{1}{n_{Aj}^s(e)} \left[ \alpha_s \left( 1 - \frac{\beta_{s1}}{2} + \frac{\beta_{s2}}{2} + \frac{\gamma_{A1}^j}{2} \right) N_{Aj}^s(\nu_e \rightarrow \nu_e) \right. \right. \\
&\quad + \alpha_s \left( 1 + \frac{\beta_{s1}}{2} + \frac{\beta_{s2}}{2} + \frac{\gamma_{A1}^j}{2} \right) N_{Aj}^s(\nu_\mu \rightarrow \nu_e) \\
&\quad + \alpha_s \left( 1 - \frac{\beta_{s1}}{2} - \frac{\beta_{s2}}{2} + \frac{\gamma_{A1}^j}{2} \right) N_{Aj}^s(\bar{\nu}_e \rightarrow \bar{\nu}_e) \\
&\quad + \alpha_s \left( 1 + \frac{\beta_{s1}}{2} - \frac{\beta_{s2}}{2} + \frac{\gamma_{A1}^j}{2} \right) N_{Aj}^s(\bar{\nu}_\mu \rightarrow \bar{\nu}_e) - n_{Aj}^s(e) \left. \right]^2 \\
&\quad + \frac{1}{n_{Aj}^s(\mu)} \left[ \alpha_s \left( 1 - \frac{\beta_{s1}}{2} + \frac{\beta_{s2}}{2} + \frac{\gamma_{A2}^j}{2} \right) N_{Aj}^s(\nu_e \rightarrow \nu_\mu) \right. \\
&\quad + \alpha_s \left( 1 + \frac{\beta_{s1}}{2} + \frac{\beta_{s2}}{2} + \frac{\gamma_{A2}^j}{2} \right) N_{Aj}^s(\nu_\mu \rightarrow \nu_\mu) \\
&\quad + \alpha_s \left( 1 - \frac{\beta_{s1}}{2} - \frac{\beta_{s2}}{2} + \frac{\gamma_{A2}^j}{2} \right) N_{Aj}^s(\bar{\nu}_e \rightarrow \bar{\nu}_\mu) \\
&\quad \left. \left. + \alpha_s \left( 1 + \frac{\beta_{s1}}{2} - \frac{\beta_{s2}}{2} + \frac{\gamma_{A2}^j}{2} \right) N_{Aj}^s(\bar{\nu}_\mu \rightarrow \bar{\nu}_\mu) - n_{Aj}^s(\mu) \right]^2 \right\} \right], \quad (3.2)
\end{aligned}$$

$$\begin{aligned}
& \chi^2_{\text{multi-GeV}} \\
&= \min_{\alpha_m, \beta', \gamma'} \left[ \frac{\beta_{m1}^2}{\sigma_{\beta m1}^2} + \frac{\beta_{m2}^2}{\sigma_{\beta m2}^2} + \frac{\gamma_1^2}{\sigma_{\gamma 1}^2} + \frac{\gamma_2^2}{\sigma_{\gamma 2}^2} \right. \\
&+ \sum_{A=L,H} \sum_{j=1}^{10} \left\{ \frac{1}{n_{Aj}^m(e)} \left[ \alpha_s \left( 1 - \frac{\beta_{m1}}{2} + \frac{\beta_{m2}}{2} + \frac{\gamma_1^j}{2} \right) N_{Aj}^m(\nu_e \rightarrow \nu_e) \right. \right. \\
&+ \alpha_s \left( 1 + \frac{\beta_{m1}}{2} + \frac{\beta_{m2}}{2} + \frac{\gamma_1^j}{2} \right) N_{Aj}^m(\nu_\mu \rightarrow \nu_e) \\
&+ \alpha_s \left( 1 - \frac{\beta_{m1}}{2} - \frac{\beta_{m2}}{2} + \frac{\gamma_1^j}{2} \right) N_{Aj}^m(\bar{\nu}_e \rightarrow \bar{\nu}_e) \\
&+ \alpha_s \left( 1 + \frac{\beta_{m1}}{2} - \frac{\beta_{m2}}{2} + \frac{\gamma_1^j}{2} \right) N_{Aj}^m(\bar{\nu}_\mu \rightarrow \bar{\nu}_e) - n_{Aj}^m(e) \left. \right]^2 \\
&+ \frac{1}{n_{Aj}^m(\mu)} \left[ \alpha_s \left( 1 - \frac{\beta_{m1}}{2} + \frac{\beta_{m2}}{2} + \frac{\gamma_2^j}{2} \right) N_{Aj}^m(\nu_e \rightarrow \nu_\mu) \right. \\
&+ \alpha_s \left( 1 + \frac{\beta_{m1}}{2} + \frac{\beta_{m2}}{2} + \frac{\gamma_2^j}{2} \right) N_{Aj}^m(\nu_\mu \rightarrow \nu_\mu) \\
&+ \alpha_s \left( 1 - \frac{\beta_{m1}}{2} - \frac{\beta_{m2}}{2} + \frac{\gamma_2^j}{2} \right) N_{Aj}^m(\bar{\nu}_e \rightarrow \bar{\nu}_\mu) \\
&+ \alpha_s \left( 1 + \frac{\beta_{m1}}{2} - \frac{\beta_{m2}}{2} + \frac{\gamma_2^j}{2} \right) N_{Aj}^m(\bar{\nu}_\mu \rightarrow \bar{\nu}_\mu) - n_{Aj}^m(\mu) \left. \right]^2 \left. \right\} \left. \right]. \quad (3.3)
\end{aligned}$$

In Eq. (3.3) we have introduced the relative normalization, which in general depends on the flavor and the energy of the events, between the upward and downward going bins:

$$\begin{aligned}
\gamma_{A1,2}^j &= \begin{cases} \gamma_{A1,2} & (j \leq j_{\text{th}}; A = L, H) \\ -\gamma_{A1,2} & (j > j_{\text{th}}; A = L, H) \end{cases} \\
\gamma_{1,2}^j &= \begin{cases} \gamma_{1,2} & (j \leq j_{\text{th}}) \\ -\gamma_{1,2} & (j > j_{\text{th}}), \end{cases}
\end{aligned}$$

and  $j_{\text{th}} = 3$  is the index which separates the upward and downward bins. The indices  $L$  and  $H$  stand for the lower ( $E < E_{\text{th}}$ ) and higher ( $E > E_{\text{th}}$ ) energy bins, and the threshold energy  $E_{\text{th}}$  is chosen so that the numbers of events for the lower and higher energy bins are approximately equal, and in the case of the sub-GeV events,  $E_{\text{th}} = 0.5\text{GeV}$ , and in the case of the multi-GeV events, the threshold energy is  $E_{\text{th}} = 3.2\text{GeV}$ , respectively, for all the zenith angle bins. We have put the systematic errors as follows:

$$\sigma_{\beta s1} = \sigma_{\beta m1} = 0.03, \sigma_{\beta s2} = 0.05, \sigma_{\beta m2} = 0.16, \sigma_\alpha = 0.2, \quad (3.4)$$

$$\sigma_{\gamma L1} = 0.005, \sigma_{\gamma L2} = 0.008, \sigma_{\gamma H1} = 0.021, \sigma_{\gamma H2} = 0.018, \sigma_{\gamma 1} = 0.015, \sigma_{\gamma 2} = 0.025. \quad (3.5)$$

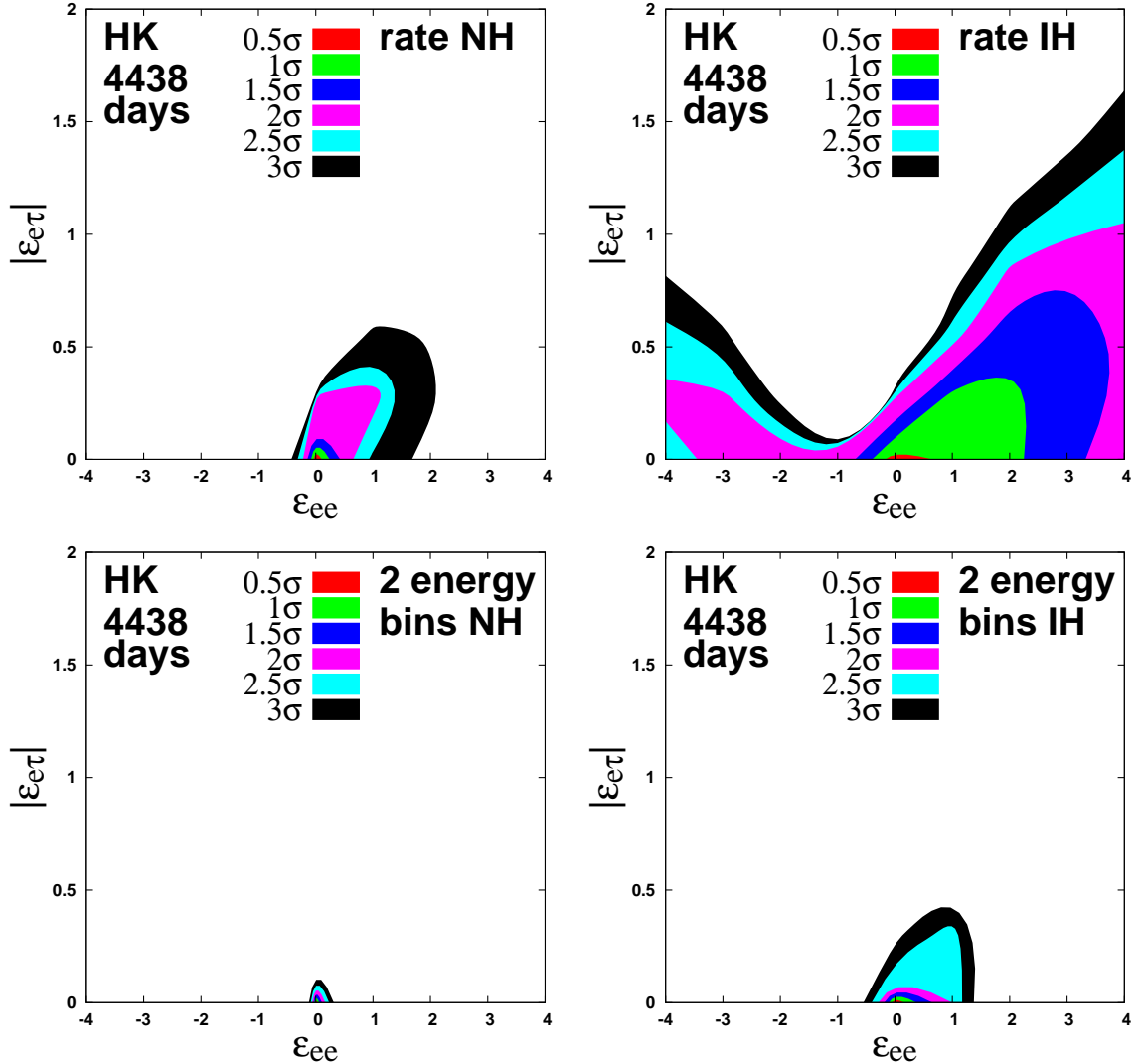


**Figure 2.** Upper panel: The allowed region in the  $(\epsilon_{ee}, |\epsilon_{e\tau}|)$  plane from the HK atmospheric neutrino data for a normal mass hierarchy (left panel) and for an inverted mass hierarchy (right panel) from the energy-rate analysis. Lower panel: The same allowed region as the upper panel from the two energy-bin analysis.

All the systematic errors in (3.4) except  $\sigma_{\beta m2}$  and  $\sigma_{\gamma 2}$  are the same as those in (2.4) in sect. 2 and those used in Ref. [51].  $\sigma_{\beta m2} = 0.16$  is the uncertainty in the relative normalization between the multi-GeV  $\nu - \bar{\nu}$  flux and it was 0.05 in (2.4).  $\sigma_{\gamma 2} = 0.025$  is the uncertainty in the relative normalization between the upward and downward going multi-GeV  $\mu$ -like events and it was 0.008 in the analysis of SK data [51]. The choice of these systematic errors (3.4) and (3.5) and the index  $j_{th} = 3$  has been made so that the result of our analysis on the mass hierarchy is close to that in Ref. [24], and we have checked that it dose not affect the sensitivity to NSI significantly.

The results from the energy rate (spectrum) analysis are given by the upper (lower)

panel in Fig. 2. From the energy rate analysis we have  $|\epsilon_{e\tau}/(1 + \epsilon_{ee})| \lesssim 0.3$  at  $2.5\sigma$ CL. On the other hand, from the energy spectrum analysis we get  $-0.1 \lesssim \epsilon_{ee} \lesssim 0.2$  and  $|\epsilon_{e\tau}| < 0.08$  at  $2.5\sigma$  (98.8%) CL for the normal hierarchy and to  $-0.4 \lesssim \epsilon_{ee} \lesssim 1.2$  and  $|\epsilon_{e\tau}| < 0.34$  at  $2.5\sigma$  (98.8%) CL for the inverted hierarchy.

From Fig. 2 we note two things. Firstly, the allowed regions from the energy spectrum analysis (the lower panel) are much smaller than those from the energy rate analysis (the upper panel) for both mass hierarchies. Secondly, the allowed regions (the right panel) for the inverted hierarchy are wider than those (the left panel) for the normal hierarchy for both rate and spectrum analyses.

To understand these phenomena, we have plotted in Fig. 3  $\chi^2_{\text{multi-GeV}}$  for the multi-GeV events, which are expected to be sensitive to the matter effect and therefore to  $\epsilon_{ee}$ , as a function of  $\epsilon_{ee}$  in the case of  $\epsilon_{e\tau} = 0$ . In plotting the figures in Fig. 3, we have taken into account only the statistical errors for simplicity, and we assume that the HK detector could distinguish neutrinos and antineutrinos for both  $e$ -like and  $\mu$ -like events in all the energy ranges of the multi-GeV events, and that the detection efficiency is the same for both neutrinos and antineutrinos. Since the SK collaboration distinguish neutrinos and antineutrinos only for the multi-GeV  $e$ -like events [47], our assumption here may not be realistic, and the separate plots for neutrinos or for antineutrinos except for the  $e$ -like events should be regarded as information for theoretical consideration. The two figures ((a) and (b)) in the top row are the results of the energy rate analysis. The two figures ((c) and (d)) in the middle row are the results of the energy spectrum analysis with two energy bins for the separate neutrino or antineutrino events. The two figures ((e) and (f)) in the bottom row are the results of the energy spectrum analysis with two energy bins of neutrinos and antineutrinos combined. Comparing the figures ((a) and (b)) in the top row and those ((e) and (f)) in the bottom row, we see that, even if some of the data set in the spectrum analysis have a sensitivity to the effect of  $\epsilon_{ee}$ , the data in the rate analysis does not necessarily have a sensitivity to  $\epsilon_{ee}$  particularly for  $\epsilon_{ee} > 0$ , for both mass hierarchies. While it is not clear to us why the sensitivity is lost only for  $\epsilon_{ee} > 0$ , we have found that, if we try to fit the same data with the numbers of events with the wrong mass hierarchy, then the plot becomes left-right reversed, i.e., the sensitivity is lost only for  $\epsilon_{ee} < 0$ . On the other hand, by comparing the figures ((c) and (d)) in the middle row and those ((e) and (f)) in the bottom row, we see that, in the case of the inverted mass hierarchy, even though the separate  $\bar{\nu}_\mu$  data has a sensitivity to  $\epsilon_{ee}$ , the combined data  $\nu_\mu + \bar{\nu}_\mu$  loses a sensitivity. We could not explain these phenomena using the analytic expression for the oscillation probability, but we interpret this loss of sensitivity as a destructive phenomenon between neutrinos and antineutrinos in the rate analysis, and between the lower and higher energy bins in the spectrum analysis for the inverted mass hierarchy.

It is expected that the HK experiment will be able to use information on the energy spectrum, so we believe that the allowed region in the lower panel in Fig. 2 with the energy spectrum analysis reflects the true HK sensitivity more than that in the upper panel does.

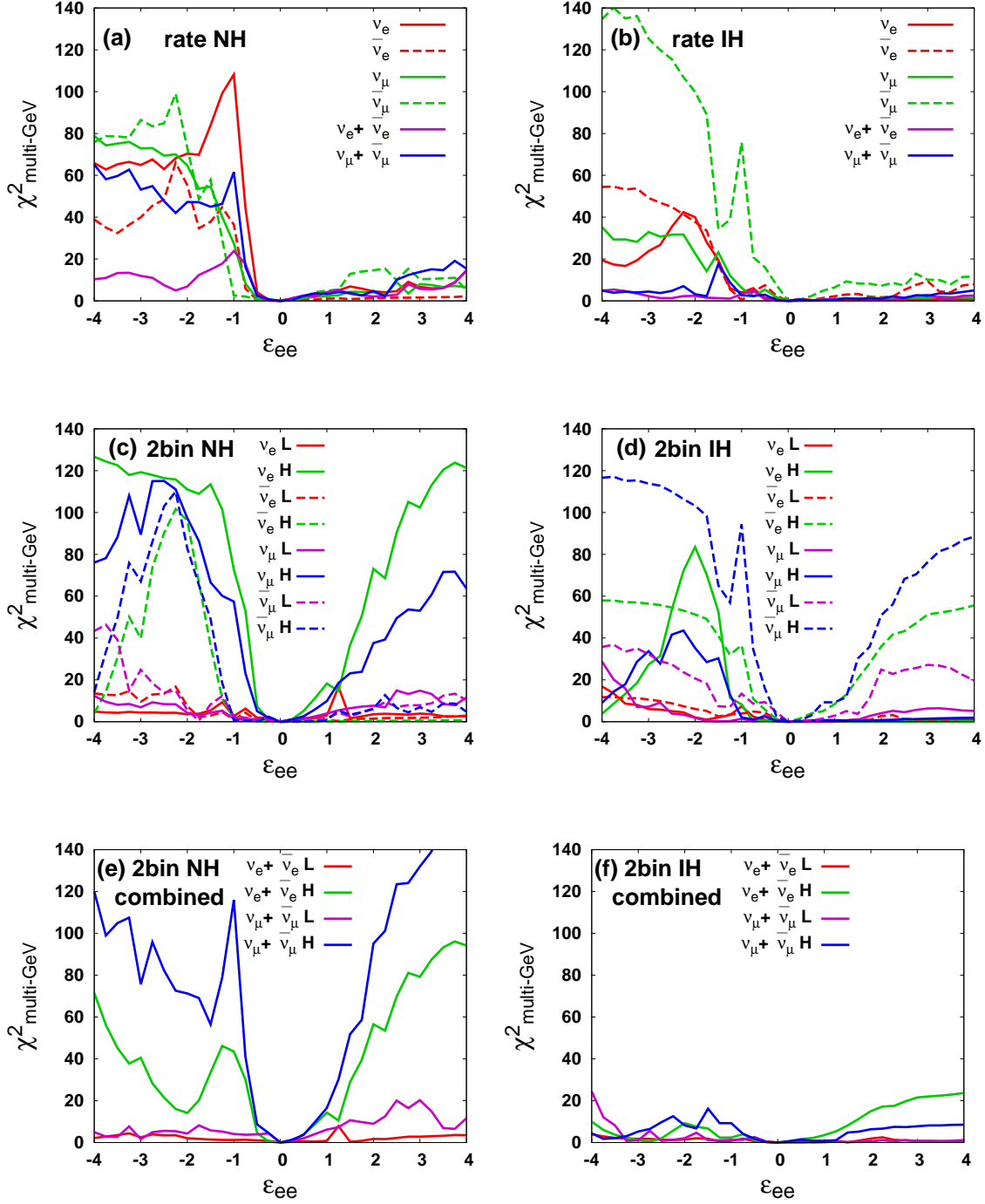


**Figure 3.** The behaviors of  $\chi^2_{\text{multi-GeV}}$  for  $\epsilon_{e\tau} = 0$  as a function of  $\epsilon_{ee}$ . (a), (b): Energy rate analysis for NH (a) and IH (b). (c), (d): Energy spectrum analysis for NH (d) and IH (e) for the separate neutrino or antineutrino events. (e), (f): Energy spectrum analysis for NH (e) and IH (f) using only the combined numbers of events of  $\nu_e + \bar{\nu}_e$  and  $\nu_\mu + \bar{\nu}_\mu$ . In (a), (b), (c) and (d), the plots for the separate neutrino or antineutrino events are created based on the assumption that HK could distinguish neutrinos and antineutrinos.

### 3.2 The case in the presence of NSI

Next let us discuss the case where “the experimental data” is the one obtained with  $(\epsilon_{ee}, \epsilon_{e\tau}) \neq (0, 0)$ . The analysis is the same as the one in subsect. 3.1, except that the “the experimental data” is produced assuming the presence of NSI, and here we perform only an energy spectrum analysis with two energy bins. The results are shown in Fig. 4, where the allowed regions at  $2.5\sigma$ CL ( $\Delta\chi^2 = 8.8$  for 2 degrees of freedom) around the true points are depicted. The straight lines  $|\epsilon_{e\tau}| = 0.8 \times |1 + \epsilon_{ee}|$  in Fig. 4 stand for the approximate bound from the SK atmospheric neutrinos in Fig. 1, and we have examined only the points below these straight lines. As seen from Fig. 4, the errors in  $\epsilon_{ee}$  and  $|\epsilon_{e\tau}|$  are small for  $|\epsilon_{ee}| \lesssim 2$  in the case of the normal hierarchy and for  $-3 \lesssim \epsilon_{ee} \lesssim 1$  in the case of the inverted hierarchy. The errors are large otherwise, and the reason that the errors are large is because a sensitivity is lost due to a destructive phenomenon between neutrinos and antineutrinos as was discussed in subsect. 3.1.

We note in passing that there are a couple of points in Fig. 4, where the allowed region has an additional isolated island. This is regarded as so-called parameter degeneracy [52–55] in the presence of the NSI. Since little is known about parameter degeneracy in the presence of the new physics and since the study of the subject is beyond the scope of this paper, we do not discuss parameter degeneracy here.

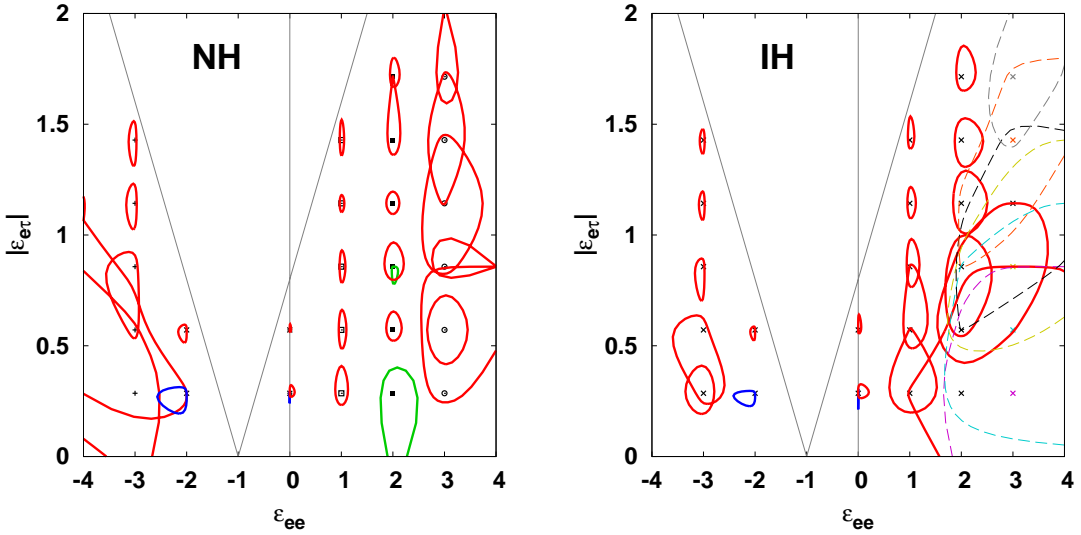


**Figure 4.** The allowed region at  $2.5\sigma$ CL around the point  $(\epsilon_{ee}, |\epsilon_{e\tau}|) \neq (0, 0)$ , where  $\bar{\delta} = \arg(\bar{\epsilon}_{e\tau}) = 0$  is assumed. Most of the allowed regions are connected, but those around a few points have an isolated island, and they are depicted with different colors. The allowed regions at  $\epsilon_{ee} = 3$  for the inverted mass hierarchy are much wider compared with other cases, so their boundary as well as their center are shown with dashed lines and with different colors.

## 4 Conclusions

In this paper we have studied the constraint of the SK atmospheric neutrino data on the non-standard flavor-dependent interaction in neutrino propagation with the ansatz (1.9). From the SK atmospheric neutrino data for 4438 days, we have obtained the bound  $|\epsilon_{e\tau}|/|1 + \epsilon_{ee}| \lesssim 0.8$  at  $2.5\sigma$ CL, while we have little constraint on  $\epsilon_{ee}$ .

We have also discussed the sensitivity of the future HK atmospheric neutrino experiment to NSI by analyses with the energy rate and with the energy spectrum. If nature is described by the standard oscillation scenario, then the HK atmospheric neutrino data will give us the bound  $|\epsilon_{e\tau}|/|1 + \epsilon_{ee}| \lesssim 0.3$  at  $2.5\sigma$ CL from the energy rate analysis, and from the energy spectrum analysis it will restrict  $\epsilon_{ee}$  to  $-0.1 \lesssim \epsilon_{ee} \lesssim 0.2$  and  $|\epsilon_{e\tau}| < 0.08$  at  $2.5\sigma$  (98.8%) CL for the normal hierarchy and to  $-0.4 \lesssim \epsilon_{ee} \lesssim 1.2$  and  $|\epsilon_{e\tau}| < 0.34$  at  $2.5\sigma$  (98.8%) CL for the inverted hierarchy. On the other hand, if nature is described by NSI with the ansatz (1.9), then HK will measure the NSI parameters  $\epsilon_{ee}$  and  $|\epsilon_{e\tau}|$  relatively well for  $|\epsilon_{ee}| \lesssim 2$  in the case of the normal hierarchy and for  $-3 \lesssim \epsilon_{ee} \lesssim 1$  in the case of the inverted hierarchy.

We have shown that it is important to use information on the energy spectrum to obtain strong constraint, because a sensitivity to NSI would be lost due to a destructive phenomena between the low and high energy events. If there is a way to distinguish between neutrinos and antineutrinos, as is done by the SK collaboration [47] for the e-like multi-GeV events, also for the multi-GeV  $\mu$ -like events, then the sensitivity to NSI would be greatly improved, because in this case we can avoid a destructive phenomena between neutrinos and antineutrinos.

While HK is expected to play an important role in measurement of  $\delta$  in the standard three-flavor scenario using the JPARC beam, HK has also a potential for new physics with atmospheric neutrinos. Search for NSI may lead to physics beyond the Standard Model, and the effects of NSI at HK deserves further studies.

## Acknowledgments

This research was partly supported by a Grant-in-Aid for Scientific Research of the Ministry of Education, Science and Culture, under Grants No. 24540281 and No. 25105009.

## References

- [1] K. A. Olive *et al.* [Particle Data Group Collaboration], Chin. Phys. C **38** (2014) 090001.
- [2] K. Abe *et al.* [Hyper-Kamiokande Working Group Collaboration], arXiv:1412.4673 [physics.ins-det].
- [3] C. Adams *et al.* [LBNE Collaboration], arXiv:1307.7335 [hep-ex].
- [4] Belle experiment, <http://belle.kek.jp/>.
- [5] Babar experiment, <http://www-public.slac.stanford.edu/babar/>.
- [6] A. Bandyopadhyay *et al.* [ISS Physics Working Group], Rept. Prog. Phys. **72**, 106201 (2009) [arXiv:0710.4947 [hep-ph]].

- [7] L. Wolfenstein, Phys. Rev. D **17**, 2369 (1978).
- [8] M. M. Guzzo, A. Masiero and S. T. Petcov, Phys. Lett. B **260** (1991) 154.
- [9] E. Roulet, Phys. Rev. D **44** (1991) 935.
- [10] S. P. Mikheev and A. Y. Smirnov, Sov. J. Nucl. Phys. **42**, 913 (1985) [Yad. Fiz. **42**, 1441 (1985)].
- [11] S. Davidson, C. Pena-Garay, N. Rius and A. Santamaria, JHEP **0303**, 011 (2003) [arXiv:hep-ph/0302093].
- [12] N. Fornengo, M. Maltoni, R. Tomas and J. W. F. Valle, Phys. Rev. D **65**, 013010 (2002) [arXiv:hep-ph/0108043].
- [13] Z. Berezhiani and A. Rossi, Phys. Lett. B **535** (2002) 207 [arXiv:hep-ph/0111137].
- [14] M. C. Gonzalez-Garcia and M. Maltoni, Phys. Rev. D **70**, 033010 (2004) [arXiv:hep-ph/0404085].
- [15] O. G. Miranda, M. A. Tortola and J. W. F. Valle, JHEP **0610**, 008 (2006) [arXiv:hep-ph/0406280].
- [16] J. Barranco, O. G. Miranda, C. A. Moura and J. W. F. Valle, Phys. Rev. D **73** (2006) 113001 [arXiv:hep-ph/0512195].
- [17] J. Barranco, O. G. Miranda, C. A. Moura and J. W. F. Valle, Phys. Rev. D **77** (2008) 093014 [arXiv:0711.0698 [hep-ph]].
- [18] A. Bolanos, O. G. Miranda, A. Palazzo, M. A. Tortola and J. W. F. Valle, Phys. Rev. D **79**, 113012 (2009) [arXiv:0812.4417 [hep-ph]].
- [19] F. J. Escrivuela, O. G. Miranda, M. A. Tortola and J. W. F. Valle, Phys. Rev. D **80**, 105009 (2009) [Erratum-ibid. D **80**, 129908 (2009)] [arXiv:0907.2630 [hep-ph]].
- [20] C. Biggio, M. Blennow and E. Fernandez-Martinez, JHEP **0908**, 090 (2009) [arXiv:0907.0097 [hep-ph]].
- [21] A. Friedland, C. Lunardini and M. Maltoni, Phys. Rev. D **70**, 111301 (2004) [arXiv:hep-ph/0408264].
- [22] A. Friedland and C. Lunardini, Phys. Rev. D **72** (2005) 053009 [arXiv:hep-ph/0506143].
- [23] H. Oki and O. Yasuda, Phys. Rev. D **82** (2010) 073009 [arXiv:1003.5554 [hep-ph]].
- [24] K. Abe, T. Abe, H. Aihara, Y. Fukuda, Y. Hayato, K. Huang, A. K. Ichikawa and M. Ikeda *et al.*, arXiv:1109.3262 [hep-ex].
- [25] G. Mitsuka *et al.* [Super-Kamiokande Collaboration], Phys. Rev. D **84** (2011) 113008 [arXiv:1109.1889 [hep-ex]].
- [26] M. C. Gonzalez-Garcia, M. Maltoni and J. Salvado, JHEP **1105** (2011) 075 [arXiv:1103.4365 [hep-ph]].
- [27] M. C. Gonzalez-Garcia and M. Maltoni, JHEP **1309** (2013) 152 [arXiv:1307.3092].
- [28] A. Friedland, C. Lunardini and C. Pena-Garay, Phys. Lett. B **594** (2004) 347 [arXiv:hep-ph/0402266].
- [29] A. Palazzo and J. W. F. Valle, Phys. Rev. D **80** (2009) 091301 [arXiv:0909.1535 [hep-ph]].
- [30] A. Friedland and C. Lunardini, Phys. Rev. D **74**, 033012 (2006) [arXiv:hep-ph/0606101].

- [31] O. Yasuda, Acta Phys. Polon. B **38**, 3381 (2007) [arXiv:0710.2601 [hep-ph]].
- [32] H. Sugiyama, AIP Conf. Proc. **981**, 216 (2008) [arXiv:0711.4303 [hep-ph]].
- [33] M. Blennow, T. Ohlsson and J. Skrotzki, Phys. Lett. B **660**, 522 (2008) [arXiv:hep-ph/0702059v3].
- [34] J. A. B. Coelho, T. Kafka, W. A. Mann, J. Schneps and O. Altinok, Phys. Rev. D **86** (2012) 113015 [arXiv:1209.3757 [hep-ph]].
- [35] A. Esteban-Pretel, J. W. F. Valle and P. Huber, Phys. Lett. B **668** (2008) 197 [arXiv:0803.1790 [hep-ph]].
- [36] M. Blennow, D. Meloni, T. Ohlsson, F. Terranova and M. Westerberg, Eur. Phys. J. C **56** (2008) 529 [arXiv:0804.2744 [hep-ph]].
- [37] J. Kopp, M. Lindner, T. Ota and J. Sato, Phys. Rev. D **77** (2008) 013007 [arXiv:0708.0152 [hep-ph]].
- [38] N. C. Ribeiro, H. Nunokawa, T. Kajita, S. Nakayama, P. Ko and H. Minakata, Phys. Rev. D **77**, 073007 (2008) [arXiv:0712.4314 [hep-ph]].
- [39] A. M. Gago, M. M. Guzzo, H. Nunokawa, W. J. C. Teves and R. Zukanovich Funchal, Phys. Rev. D **64** (2001) 073003 [arXiv:hep-ph/0105196].
- [40] T. Ota, J. Sato and N. a. Yamashita, Phys. Rev. D **65** (2002) 093015 [arXiv:hep-ph/0112329].
- [41] P. Huber, T. Schwetz and J. W. F. Valle, Phys. Rev. Lett. **88** (2002) 101804 [arXiv:hep-ph/0111224].
- [42] M. Campanelli and A. Romanino, Phys. Rev. D **66** (2002) 113001 [arXiv:hep-ph/0207350].
- [43] N. C. Ribeiro, H. Minakata, H. Nunokawa, S. Uchinami and R. Zukanovich-Funchal, JHEP **0712** (2007) 002 [arXiv:0709.1980 [hep-ph]].
- [44] J. Kopp, T. Ota and W. Winter, Phys. Rev. D **78** (2008) 053007 [arXiv:0804.2261 [hep-ph]].
- [45] A. M. Gago, H. Minakata, H. Nunokawa, S. Uchinami and R. Zukanovich Funchal, JHEP **1001**, 049 (2010) [arXiv:0904.3360 [hep-ph]].
- [46] D. Meloni, T. Ohlsson, W. Winter and H. Zhang, arXiv:0912.2735 [hep-ph].
- [47] K. Abe *et al.* [Super-Kamiokande Collaboration], arXiv:1410.2008 [hep-ex].
- [48] R. Foot, R. R. Volkas and O. Yasuda, Phys. Rev. D **58** (1998) 013006 [hep-ph/9801431].
- [49] O. Yasuda, Phys. Rev. D **58** (1998) 091301 [hep-ph/9804400].
- [50] O. Yasuda, hep-ph/0006319.
- [51] Y. Ashie *et al.* [Super-Kamiokande Collaboration], Phys. Rev. D **71**, 112005 (2005) [arXiv:hep-ex/0501064].
- [52] J. Burguet-Castell, M. B. Gavela, J. J. Gomez-Cadenas, P. Hernandez and O. Mena, Nucl. Phys. B **608**, 301 (2001) [arXiv:hep-ph/0103258].
- [53] H. Minakata and H. Nunokawa, JHEP **0110**, 001 (2001) [arXiv:hep-ph/0108085].
- [54] G. L. Fogli and E. Lisi, Phys. Rev. D **54** (1996) 3667 [arXiv:hep-ph/9604415];
- [55] V. Barger, D. Marfatia and K. Whisnant, Phys. Rev. D **65**, 073023 (2002) [arXiv:hep-ph/0112119].